AME0002
Study on Effectiveness of Frontal Crash Standards for Passenger Bus using Finite Element Analysis

Burawich Muangto[1,*], Pattaramon Jongpradist[1]

[1] Department of Mechanical Engineering, Faculty of Engineering, King's Mongkut's University of Technology Thonburi
126 Pracha-uthit Rd., Bangmod, Thungkru, Bangkok 10140, Thailand
[*] Corresponding Author: burawichmuangto@gmail.com, +668-9691-0190

Abstract

Frontal impact is among the major causes of severe accidents occurred with passenger bus. Two standard procedures for frontal collision integrity are universally adopted; Economic Commission for Europe Regulation 29 (ECE-R29) in which a 1,500-kg rigid pendulum strikes the bus frontal structure with 55-kJ impact energy, and Federal Motor Vehicle Safety Standard 208 (FMVSS-208) in which the bus structure crashes to a rigid barrier at the velocity of 30 km/h. This study aims to use nonlinear explicit finite element method to analyze the safety of the driver of passenger bus manufactured in Thailand according to ECE-R29 and FMVSS-208 standards and compare the results between the two regulations. A finite element model of bus structure is developed and analyzed for the driver velocities during crash. A hybrid III 50th percentile dummy driver is employed in Hypercrash to predict severity of head and neck injury after impact tests. Comparisons between the two standards include the absorbed energy in each structure section, deformation of A-pillars, injury and protection of the driver. Also, the critical points in design of bus frontal structure are discussed and design improvement is recommended.

***Keywords**:* Frontal Impact, Bus safety, ECE-R29, FMVSS-208, Injury mechanism

1. Introduction

Road accidents can be divided into four types including frontal collision, side impact, rear-end impact and rollover [1]. Accident statistics from the Traffic Safety Facts 2014 report presented the numbers of vehicle accident, fatality and injury rates per vehicle during the past years. The major share for initiation point of fatal bus accidents in USA of forty percent is reported to be the results of frontal impact [2].

In bus frontal impact, the key factor to fatal accidents resulting in high risk of passenger safety is when the driver cannot control the bus because of his severe injury or fatality. Standards for frontal impact of heavy vehicle are therefore not only related to the strength of structure for passenger safety but also the injury of the bus driver so as to mitigate accident severity. Two standard procedures for frontal collision integrity are widely adopted, i.e., Economic Commission for Europe Regulation 29 (ECE-R29) [3] and Federal Motor Vehicle Safety Standard 208 (FMVSS-208) [4].

The ECE-R29 regulation has been used to examine the strength of bus and coach frontal structures via finite element method and determine the critical sections for structural improvement [5,6]. Guosheng et al. [7] used LS-DYNA to analyse the impact test of pendulum and fixed barrier wall according to ECE-R29 and ECE-R94 for passenger bus. Experiments were performed with several test dummy models. It was found that three-point safety belt is necessary for safety of the driver under frontal crash. Youming et al. [8] analysed the deformation of bus frontal frame following the regulations ECE-R29 and FMVSS-208. Structural deformation of driver window and right door areas are excessive. Moreover, cabin deformation from FMVSS-208 impact test are much greater than those from ECE-R29 pendulum test. There are limited studies that directly consider occupant responses and injuries. Li et al. [9] used Hybrid III 50th percentile dummy to analyze occupant injuries in Ford F250 crashes into roadside barriers by using Finite Element Analysis. Passenger injuries were estimated using criteria based directly on dummy responses and compared to those based on vehicle responses. In such cases, some discrepancies were observed.

In earlier research, frontal impact of bus structures was studied to investigate structural responses such as the maximum deformations of the bus frontal structure but did not evidently compare the safety criteria on the driver injury risk of the two standards. This research aims to employ nonlinear explicit finite element analysis to investigate the absorbed energy in each structural section, deformations of A-pillars and injury mechanism of the driver dummy according to frontal impact standards ECE-R29 and FMVSS-208.

2. Frontal impact standards

The frontal impact standards widely enforced for passenger bus including ECE-R29 and FMVSS-208 are explained below.

2.1 ECE-R29 standards

ECE-R29 is a frontal crash test standard recommended by United Nations (UN). There are 3 types of impact test, i.e., Test A, Test B and Test C. Test A is intended to evaluate the resistance of a cab in frontal impact accident. Test B is an impact test to the

A-pillar of the cab and Test C is a cab roof strength test. This paper focuses on the analysis of driver safety during frontal impact accident. Thus, the bus model is analyzed based on Test A.

According to frontal impact test in ECE-R29 Test A, the vehicle is striked by a pendulum of impact energy 55 kJ. The pendulum plate has a surface of 2500 mm × 800 mm and made of steel with evenly distributed mass not less than 1500 kg. The pendulum is suspended by two rigid beams of 1000 mm apart and 3500 mm between axis point of suspension and geometric center of the impactor surface. Its striking surface shall be in contact with the front part of the vehicle at 50 mm below the R-point of the driver's seat as shown in Fig. 1. To meet the requirement, there should be no contact between the driver manikin and the non-resilient parts of the bus structure after the impact.

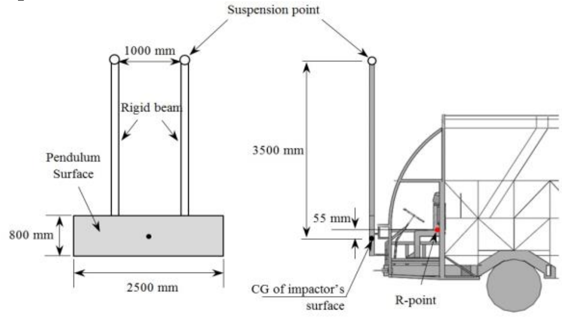

Fig. 1 Front impact test according to ECE-R29 Test A

2.2 FMVSS 208 standard

FMVSS-208 is a frontal crash test standard recommended by National Highway Traffic Safety Administration (NHTSA) in United States of America. The tests include full, oblique and offset frontal impact to a rigid barrier or deformable barriers. Head-on full frontal impact with a fixed barrier is similar to the real frontal crash accident and thus is widely used to analyze the strength of front member of vehicles.

According to the standard, the velocity of 23 to 48 km/h is applied to the passenger bus traveling longitudinally forward into a rigid barrier as illustrated in Fig. 2.

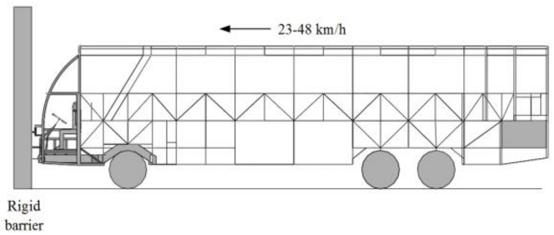

Fig. 2 Head-on full frontal fixed barrier

The requirements for FMVSS-208 are based on injury of the driver as following:

- Head Injury Criteria (HIC) is a measure of the likelihood of head injury calculated by the dummy's head acceleration defined as

$$\mathrm{HIC} = \max\left(\frac{1}{t_2 - t_1}\int_{t_1}^{t_2} a(t)dt\right)^{2.5}(t_2 - t_1) \qquad (1)$$

where t_1 and t_2 are the initial and final time instances of the interval attaining the maximum HIC and $a(t)$ is acceleration measured in term g (gravity acceleration) at any time.

A HIC_{15} (the impact interval over 15 ms) of 700 represents a 5 percent risk of injury [10] while HIC_{36} score of 1000 gives 18 percent probability of a severe head injury [11].

- Neck Injury Criteria (Nij) is an indicator for tolerance limits of a linear combination of axial load and bending moment of neck injury calculated by

$$\mathrm{Nij} = \frac{F_y}{F_{\mathrm{int}}} + \frac{M_y}{M_{\mathrm{int}}} \qquad (2)$$

where F_y is axial load, F_{int} is the critical intercept value of load used for normalization, M_y is the flexion/extension bending moment and M_{int} is the critical intercept value for moment used for normalization. To pass the standard, Nij must not be greater than one at any time during the event.

- Force transmitted axially through upper leg is not greater than 10kN.
- Tension in upper neck is not greater than 4,170 N.
- Compression in upper neck is not greater than 4,000 N.

3. Computational Models

This section describes the finite element models of bus structure, loading conditions according to ECE-R29 and FMVSS-208 and the driver dummy model used in this work.

3.1 Finite element model for bus structure

The passenger bus model in this study has the dimensions of 2.52 m wide, 14.5 m long, 3.25 m high that carries 42 passengers as shown in Fig. 3. The bus body frame are made from steel rectangular cross sections of 50×50×2.3 mm and 50×25×2.3 mm. The material density is 7,860 kg/m^3. The elastic modulus is 210 GPa and Poisson's ratio is 0.3. The chassis is made of structural steel with yield strength 570 MPa and ultimate strength 650 MPa while other parts are made of mild steel with yield strength and ultimate strength of 330 MPa and 375 MPa, respectively. The total weight of the bus frame is 3.51 tons. The front parts of the bus body are meshed with 55,652 4-noded shell elements while the other parts are modeled with 11,160 beam elements. The mesh size is chosen to be 5 to 25 mm where the deformations are large whereas the 60 mm element size is applied to other parts. A rigid driver dummy is fixed on the floor plate at driver position to capture the imposed velocity from the crash.

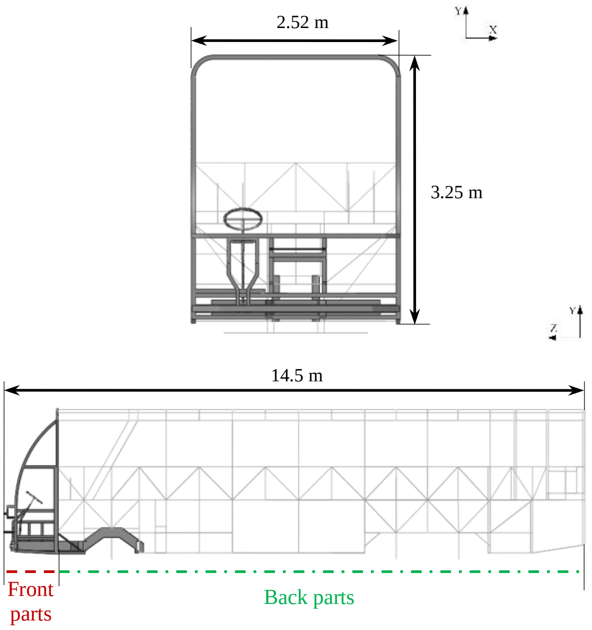

Fig. 3 Bus structure model

3.2 ECE-R29 Model

In ECE-R29 model, the bus structure is placed on a rigid floor with surface to surface interactions where the friction coefficient between tires and floor is 0.7. The tires are chained to the floor to restrain the bus movement during impact. Surface to surface contact interaction is assigned to the pendulum and front parts of bus structure. Self-contact interactions of the bus members are also employed. The angular velocity applied to the pendulum is obtained from

$$E = \frac{1}{2} I_{xx} \omega_x^{\ 2} \tag{3}$$

where E is the impact energy, I_{xx} is the mass moment of inertia of the pendulum about x-axis at pivot point equal to 20717 kg/m^3. Therefore, the initial angular velocity of the pendulum to create strike impact of 55 kJ is 2.306 rad/s as shown in Fig. 4.

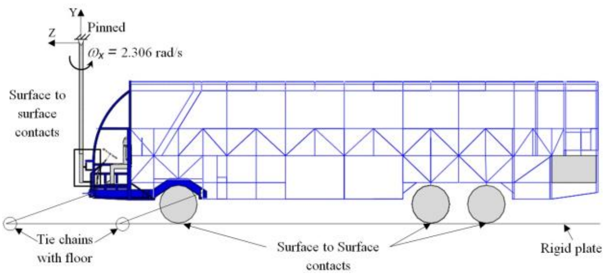

Fig. 4 ECE- 29 model

3.3 FMVSS 208 Model

For FMVSS-208 FE model, the initial velocity of 30 km/h forward to a fixed rigid barrier is applied. The bus model and contact interactions are assigned similar to those of ECE-R29 model without the chain connections as depicted in Fig. 5.

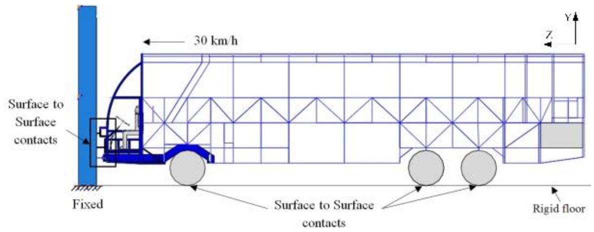

Fig. 5 FMVSS 208 model

3.4 FE Model for driver dummy

The finite element model of the driver dummy is Hybrid III 50th percentile Male with the total weight of 78 kg [12] imported from Hypercrash. The dummy consists of 5,004 shell elements and 25 spring elements. The seat cushion and headrest are made of visco-elastic polyurethane close cell foam with density 100 kg/m^3 and Young's modulus of 15 MPa.

Fig. 6 shows the dummy model used in the simulation and the positions of injury measurement sensors, that is, head, neck and upper legs. The dummy is placed on the cushions with multi-usage contact interface and cushions are tied to the seat frame. Node-to-surface contact interface is assigned to the head and headrest while self-impact interface is assigned to the cushion and headrest. The initial and imposed velocities in three directions of the driver are obtained from the structural analyses according to ECE-R29 and FMVSS-208 models and they are imposed to the dummy.

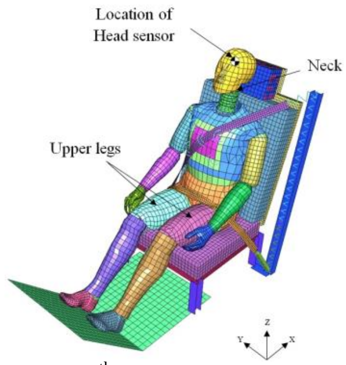

Fig. 6 Hybrid III 50th percentile driver dummy model

4. Results and Discussions

Two frontal crash problems are simulated by dynamic explicit finite element analysis following ECE-R29 and FMVSS-208 standards.

4.1 Deformation shape after impact

The deformed shapes of the bus at different time instances are shown in Figs. 7 and 8. From the deformed shapes of the bus, it is obvious that the impact from FMVSS 208 is more severe and the imposed collision energy from impact is considerably more than that from ECE R29. For both regulations, A-pillars are largely deformed after impact as shown in Fig. 9. Solid lines are deformations from ECE-R29 and dashed lines are values for FMVSS 208.

AME0002

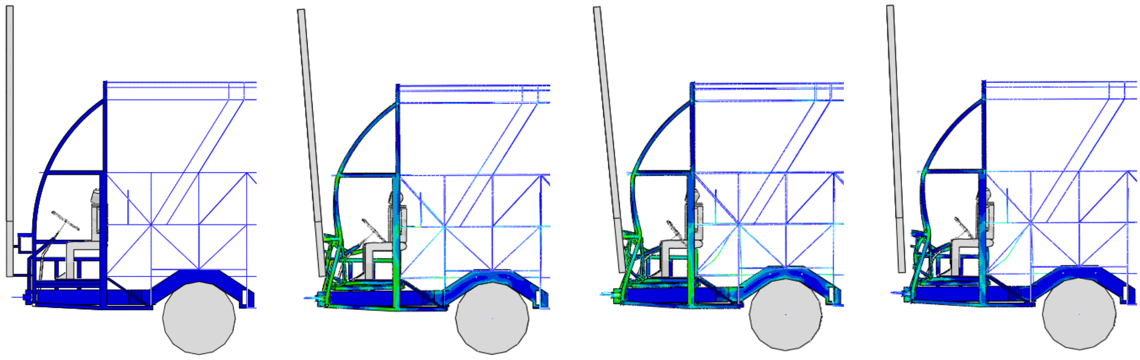

(a) t = 0 ms Impact instant | (b) t = 45 ms During impact | (c) t = 80 ms Max.A-pillar deformation | (d) t = 200 ms After impact

Fig. 7 Deformation shapes at different time instances of ECE-R29

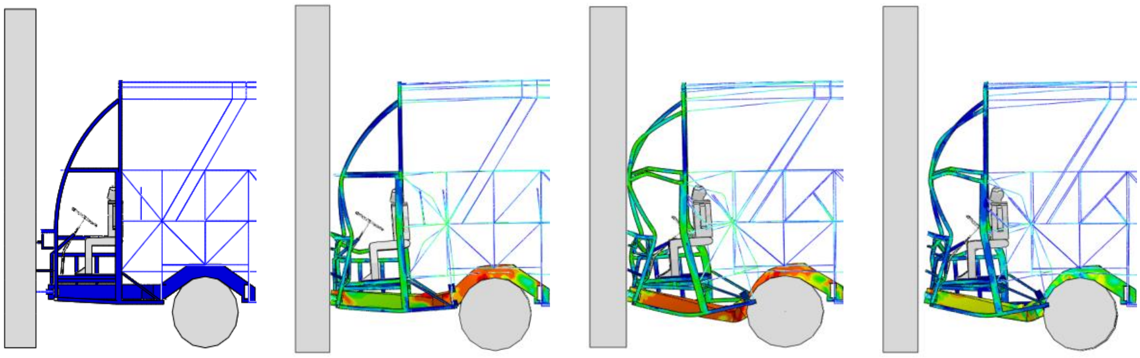

(a) t = 0 ms Impact instant | (b) t = 45 ms During impact | (c) t = 155 ms Max.A-pillar deformation | (d) t = 400 ms After impact

Fig. 8 Deformation shapes at different time instances of FMVSS-208

The maximum deformations of A-pillars for both FMVSS-208 and ECE-R29 models occur to the left pillar because no bracing member is present on the left side frame at the driver's door. The bracing beam at the window on the right pillar also causes smaller deformation at the middle part of the right pillar. Most deformations of A-pillar in ECE-R29 model happens only at the pendulum impact area while outward bending is observed at the upper part of A-pillar of FMVSS-208 model. From Figs. 7 and 8, it can be noticed that the steering systems in both models are in contact with the driver manikins. Therefore, the bus structure does not pass the requirement of ECE-R29 regulation that no contact between the driver and non-resilient parts of the bus should occur.

At the driving position as displayed in Fig. 10, the clearances between the steering system and the driver's knee (c_1), chest (c_2) and lap (c_3) are 176 mm, 175 mm and 160 mm, respectively. In ECE-R29 model, the pendulum surface impacts directly to the R-point and causes the steering system to trespass into the driver manikin more than FMVSS-208 regulations as shown in Table. 1. Negative clearances mean the steering system intrudes into the driver dummy.

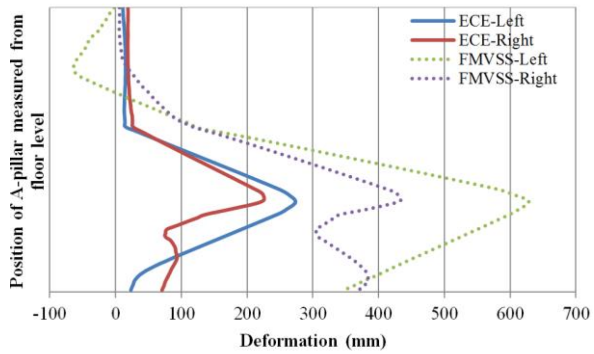

Fig. 9 Deformation of A-pillar after impact

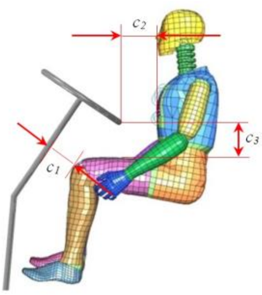

Fig. 10 Clearances between driver and steering system

Table. 1 Minimum clearance between the steering system and the driver manikin

Clearances(mm)	ECE-R29	FMVSS-208
c_1	-71	-44
c_2	-25	-20
c_3	-100	-20

4.2 Energy absorption

Trends of energy plots during impact for both standard tests are similar as shown in Fig. 11. The total energy is constant during impact illustrate suitable simulation and reliable results. Kinetic energy starts at maximum and decreases when the energy is absorbed and dissipated as internal strain energy in terms of plastic deformation of structure.

Comparisons of energy absorption in each structure section between ECE-R29 and FMVSS 208 are shown in Table. 2. The major portion in energy absorption of 78.9% occurs at cabin section in ECE-R29 whereas 63.7% is absorbed by the back section in FMVSS-208 model. In ECE-R29 model, the pendulum crashes into the crumple section first and the crash energy subsequently dissipates to cabin and back section of bus structure. Since the pendulum does not directly strike at the chassis position, less energy is transferred through chassis to the back part of the bus structure.

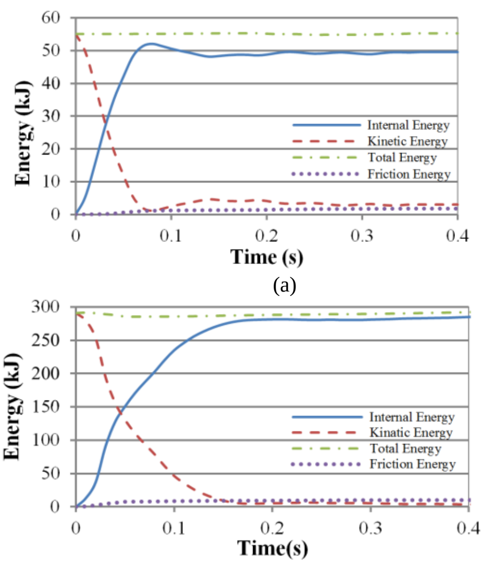

(b)

Fig. 11 Energy plot during impact simulation (a) ECE-R29 regulation and (b) FMVSS-208 regulation

Table. 2 Percentage of energy absorption in each structure

Section	ECE-R29		FMVSS-208	
	EA (kJ)	Rate (%)	EA (kJ)	Rate (%)
Whole structure	52.1	100.0	249.9	100.0
Crumple structure	5.9	11.3	3.9	1.6
Cabin structure	41.1	78.9	86.8	34.7
Back structure	5.1	9.8	159.2	63.7

Moreover, it can be noticed that crumple structure can merely absorb little energy. Most of the impact energy is absorbed by the cabin section and therefore, large deformation arises in this part. In the case of FMVSS-208 regulation, the front section of the bus is in contact with the rigid barrier wall. Energy transfers through the chassis to the back section and thus this part absorb the most energy from collision.

From the percentage of energy absorption in each structure for both cases, it is apparent that crumple structure absorbs only small amount of impact energy compared with other sections. hence, the design of crumple structure should be improved to effectively absorb the crash energy through its plastic deformation.

4.3 Dummy velocity and acceleration

The velocity of the driver dummy after frontal impact regarding simulation of ECE-R29 and FMVSS 208 models are shown in Fig. 12. The obtained velocities are then imposed to the driver dummy in Hypercrash and solve for the forces and moments in each sensor via RADIOSS solver. The head acceleration in term g during impact is depicted in Fig. 13. The maximum acceleration at the head position based on ECE-R29 and FMVSS-208 are 40.1g and 71.7g, respectively. The maximum axial force and maximum moment in the upper neck from ECE-R29 model are equal to 768.3 N of tension and 49.7 N.m of flexion. For FMVSS-208 model, the maximum tension force is 1807.7 N and the maximum flexion is 181.4 N.m. Fig. 14 shows the boundaries of allowable Nij axial force and bending moment, and the values obtained from simulation. It can be seen that the injuries at the neck of the dummy from both models are less than the allowable value which means the neck injury of the driver after impact is not severe. The neck injury according to FMVSS 208 model is more than that from ECE R29 because of the high value of deceleration during impact especially in x-direction and Nij is at the upper bound limit.

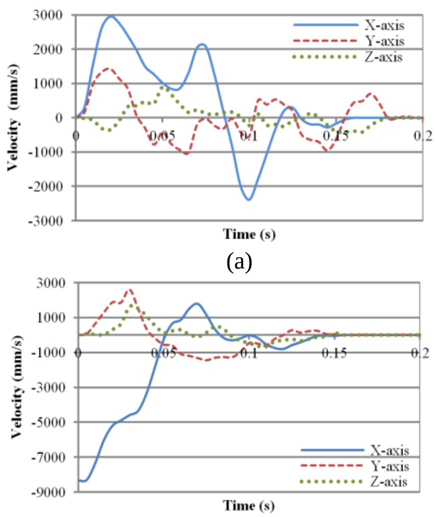

(b)

Fig. 12 Imposed velocity of (a) ECE-R29 Model (b) FMVSS 208 Model

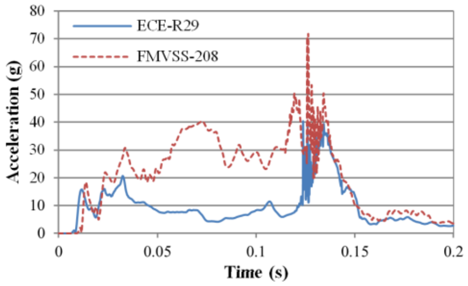

Fig. 13 Head acceleration in term g during impact

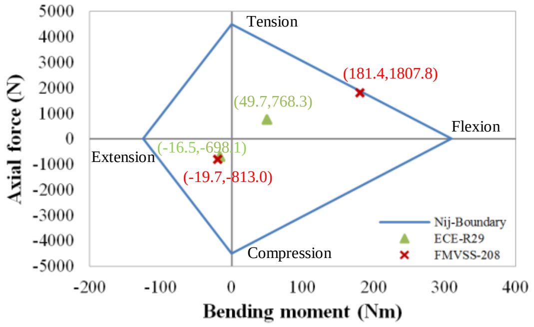

Fig. 14 Nij-boundary for axial force and bending moment

Table. 3 Results of injury severity of the dummy

Injury	ECE-R29	FMVSS-208	Limit
HIC_{15}	64.1	140.4	700
HIC_{36}	66.7	265.3	1,000
Nij	0.33	0.98	1
Upper leg Force (kN)	1.12	2.41	10
Upper neck Tension (N)	768	1,808	4,175
Upper neck Compression (N)	698	813	4,000

Table. 3 listed the results of dummy injuries based solely on the dummy velocities without considering intrusion of the steering system into the dummy. The injury score of the driver dummy according to ECE-R29 model is lower than that tested based on FMVSS-208. However, both models pass all the injury requirements stated in FMVSS 208 whereas both do not pass the ECE-R29 regulation. Thus, one of the important part to be enhanced in design for protection of the driver under frontal collision is reinforcement of frontal structure correlating to the deformation of steering system after impact.

5. Conclusions

This paper implements nonlinear explicit finite element method to examine crashworthiness of bus structure and driver's injury index for a passenger bus manufactured in Thailand based on ECE-R29 and FMVSS-208 regulations. The bus structure does not pass ECE-R29 requirement due to intrusion of the steering system into the driver manikin but the injury score of the driver can pass the conditions in FMVSS-208 regulation. The impact energy from FMVSS-208 model is almost four time more than that of ECE-R29 and distributions of absorbed energy in structural part are also different. Proper design of crumple section can improve energy dissipation to reduce deformation of A-pillars and other critical sections. Though, when the driver's injuries are considered, both models can pass FMVSS regulation. To improve the bus design, the crumple zone with energy absorbers should be installed and reinforcement relating to displacement of steering system should be concerned.

6. Acknowledgement

The authors gratefully acknowledge the 2015 Mitsui Sumitomo Insurance Welfare Foundation Research Grant (MSIWF).

7. References

[1] Hesham, K. (2009). Design Optimization of Vehicle Structures for crashworthiness Improvement. Dissertation, Mechanical and Industrial Engineering Faculty, Concordia University, Canada.

[2] National Highway Traffic Safety Administration (2014), Traffic safety facts 2014, A Compilation of Motor Vehicle Crash Data from the Fatality Analysis Reporting System and the General Estimates System, Washington DC.

[3] United Nations (2011), Economic Commission for Europe agreement regulation No. 29, Uniform Provisions Concerning the Approval of Vehicles with regard to the Protection of the Occupants of the Cab of a Commercial Vehicle.

[4] Legal Information Institute Standard No. 208; *Occupant crash protection*, URL: https://www.law.cornell.edu/cfr/text/49/571.208, accessed on 20/12/2015.

[5] Cerit, E., Guler, A., Bayram, B., and Yolum, U. (2010), Improvement of the Energy Absorption Capacity of an Intercity Coach for Frontal Crash Accident, *International ls-dyna users conference*, June 6-8, Michigan, U.S.A., pp 15-24.

[6] Jongpradist, P., Senawat, S. and Muangto, B. (2015), Improvement of Crashworthiness of Bus Structure under Frontal Impact, *2015 World Congress on Advances in Structural Engineering and Mechanics (ASEM15)*, 25-29 August, Incheon, Korea.

[7] Guosheng, Z., Yang, W., Qiang, L. and Zicheng, L. (2014), Occupant Risk Evaluation Based on Frontal Collision of Bus, *International Conference on Logistics Engineering Management and Computer Science (LEMCS 2014)*, May 24-26, 2014, Shenyang, China, pp. 1103-1106.

[8] Youming, T., Yongpan, Y. and Hongwu, H. (2013), Energy Absorption Study on Drive Cab of an Intercity Coach in Frontal Impact Analysis, *2013 Fifth International Conference on Measuring Technology and Mechatronics Automation*, January 16-17, 2013, Hong Kong, China, pp. 520-523.

[9] Li, N., Fang, H., Zhang, C., Gutowski, M., Palta, E. and Wang, W. (2015), A numerical study of occupant

AME0002

responses and injuries in vehicular crashes into roadside barriers based on finite element simulations, Advances in Engineering Software, Volume 90, December 2015, pp. 22-40.

[10] Mertz, H., Prasas, P., and Irwin, A. (1997). Injury Risk Curves for Children and Adults in Frontal and Rear Collisions in *the 41st Stapp Car Crash Conference*, Warrendale, PA

[11] Kuppa, S. and Saul, R. (1999). Development of Improve Injury Criteria for the Assessment of Advanced Automotive Restraint Systems-II, Vehicle Research and Test Center (VRTC).

[12] Humanetics innovative solutions; *Hybrid III 50th Male Dummy*, URL: https://www.humaneticsatd.com /crash-test-dummies/frontal-impact/hybrid-iii-50th, accessed on 12/02/2016.